# Precision Measurement of the Hydrogen-Deuterium $1S - 2S$ Isotope Shift

Christian G. Parthey,[1] Arthur Matveev,[1] Janis Alnis,[1] Randolf Pohl,[1] Thomas Udem,[1] Ulrich D. Jentschura,[2] Nikolai Kolachevsky,[1,*] and Theodor W. Hänsch[1,†]

[1]*Max-Planck-Institut für Quantenoptik, 85748 Garching, Germany*

[2]*Department of Physics, Missouri University of Science and Technology, Rolla, Missouri 65409, USA*

(Received 15 April 2010; published 7 June 2010)

Measuring the hydrogen-deuterium isotope shift via two-photon spectroscopy of the $1S - 2S$ transition, we obtain 670 994 334 606(15) Hz. This is a 10-times improvement over the previous best measurement [A. Huber *et al.*, Phys. Rev. Lett. **80**, 468 (1998)] confirming its frequency value. A calculation of the difference of the mean square charge radii of deuterium and hydrogen results in $\langle r^2\rangle_d - \langle r^2\rangle_p = 3.820\,07(65)\ \mathrm{fm}^2$, a more than twofold improvement compared to the former value.

DOI: 10.1103/PhysRevLett.104.233001 PACS numbers: 06.20.Jr, 31.30.jc, 32.30.Jc

Today, precision atomic spectroscopy is the most powerful tool to study the root mean square charge radius of simple nuclei. The simplest compound nucleus, the deuteron, is of great interest to test nuclear few-body physics. Historically, its charge radius has been determined by scattering experiments [1], until precision measurements of the hydrogen-deuterium (H-D) $1S - 2S$ isotope shift became competitive [2–4]. Although the nuclear-size corrections to the electronic energy levels are as small as $10^{-9}$ in relative units, they contribute with the largest uncertainty to the theoretical description within the framework of QED. Therefore, the charge radii (or differences) may be extracted from absolute frequency measurements (or isotope shifts). These determinations rely on the correctness of QED calculations.

To allow the determination of the charge radii *and* simultaneously verify the predictions of QED, a measurement of the $2S$ Lamb shift in muonic hydrogen ($\mu p$) has been conducted recently [5]. With the same nucleus as in ordinary hydrogen but with an orbiting lepton that is $\sim 200$ times heavier, the finite-size correction in this system is $\sim 200^3$ larger. Previous results obtained from H spectroscopy, as expressed by the CODATA [6] value for the proton mean square charge radius $\langle r^2\rangle_p$, differ significantly from the recent value obtained from $\mu p$. This provides motivation for an improved measurement of the H-D isotope shift. Furthermore, it stimulates theoretical discussions about the interpretation of the charge radius [7,8], the consistency of the electron scattering data with spectroscopy experiments, and calculations of the deuteron polarizability [9].

Here, we present a measurement of the H-D isotope shift based on two-photon spectroscopy of the $1S - 2S$ transition which has a natural line width of 1.3 Hz. We excite the magnetic field insensitive hyperfine transitions $F = 1 \rightarrow 1$, $m_F = \pm 1 \rightarrow \pm 1$ in H and $F = \frac{3}{2} \rightarrow \frac{3}{2}$, $m_F = \pm\frac{3}{2} \rightarrow \pm\frac{3}{2}$ in D. The isotope shift of the $1S - 2S$ hyperfine centroid is given by the difference of the transition frequencies $\Delta f_{\mathrm{exp}} = f^{\mathrm{D}}_{1S-2S} - f^{\mathrm{H}}_{1S-2S} - \Delta f_{\mathrm{HFS}}$, where the hyperfine structure correction $\Delta f_{\mathrm{HFS}} = 215\,225\,596.5(2.9)$ Hz has been calculated from the hyperfine splitting measured in experiments [10–13]. Two data runs in March and April 2009 (first run) and August 2009 to January 2010 (second run) were recorded. A diode laser and a dye laser were used for H and D in the first run, respectively [see Fig. 1(a)], whereas in the second run, both isotopes were excited by the diode laser system [see Fig. 1(b)].

The laser system used for hydrogen spectroscopy is a frequency quadrupled master oscillator power amplifier seeded by a 20 cm long extended cavity diode laser at 972 nm (ECDL1) which is tuned to the eighth subharmonic of the $1S - 2S$ transition. The laser frequency is stabilized

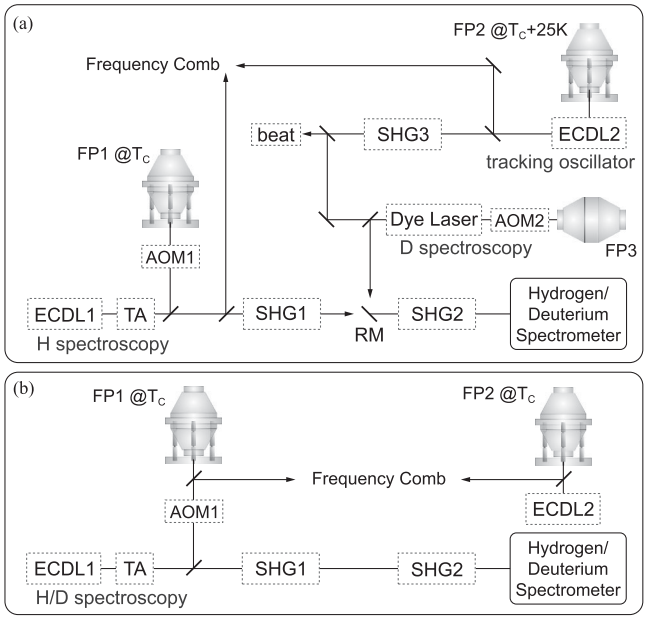


FIG. 1. Schematic of the laser system. Setup (a) was used during the first nine days of measurement. For the second run, setup (b) was used. ECDL stands for extended cavity diode laser, FP for Fabry-Perot cavity, $T_c$ for zero expansion temperature, SHG for second harmonic generation stage, TA for tapered amplifier, and RM for removable mirror.

 

to a transmission peak of a vibrationally and thermally isolated high finesse cavity (FP1) made from ultralow expansion glass (ULE). The cavity is stabilized at its zero expansion temperature $T_c$, which greatly reduces its temperature sensitivity [14]. The laser is continuously kept in lock during each measurement day showing an almost linear frequency drift of $+50$ mHz/s. The spectral line width of the laser measured after the tapered amplifier is less than 0.5 Hz and its relative frequency instability reaches $4 \times 10^{-15}$ in $10^3$ s. To scan over the atomic transition the frequency of ECDL1 is shifted in steps by a double pass acousto-optic modulator (AOM) installed between FP1 and ECDL1. The actual laser frequency is measured by an Er-doped fiber frequency comb referenced to an active, Global Positioning System (GPS) disciplined hydrogen maser. According to its specification, the fractional frequency instability of the maser is lower than $2 \times 10^{-15}$ on the time interval from $10^3$ to $10^5$ s. GPS calibration provides a frequency inaccuracy of less than $5 \times 10^{-15}$. For our differential frequency measurement the frequency stability of the reference is much more important than its accuracy. The lowest uncertainty for $\Delta f_{\mathrm{exp}}$ is reached when $f^{\mathrm{D}}_{1S-2S}$ and $f^{\mathrm{H}}_{1S-2S}$ are measured within one day.

The $1S - 2S$ transition in atomic deuterium was excited with the second harmonic of a dye laser at 486 nm locked to a spring-suspended ULE cavity in a horizontal configuration (FP3). The laser has an irregular frequency drift of $<1$ Hz/s and a line width of 60 Hz measured over 0.2 s. The second diode laser ECDL2, which is continuously locked to the FP2 ULE cavity, was used as a transfer oscillator between the frequency comb and the dye laser. In the first run all beat notes were counted using HP/Agilent 53131A counters. All counters and synthesizers are referenced to the H-maser.

In the second run we use ECDL1 as the spectroscopy laser for both isotopes [see Fig. 1(b)]. This is advantageous since its almost perfectly linear drift allows us to fit its beat frequency with the comb by a straight line. This allows a more accurate averaging of the maser noise as compared to the segment-wise parabolic fit used to approximate the nonlinear drift of FP2. ECDL2 with FP2 is only used to monitor the correct operation of ECDL1 through a transfer beat via the frequency comb [15]. Instead of measuring the actual laser frequency we measure the frequency of the light coupled to the cavities, decoupling the frequency determination from the spectroscopy. In the second run, all frequencies are counted with Klische + Kramer FX-80 continuous counters.

The excitation and detection configuration are similar to those used in previous experiments [16] (see Fig. 2). Molecular hydrogen and deuterium are purified in separate Pd filters and dissociated in a microwave discharge running in a sapphire tube at a pressure of 0.7–3.4 mbar set by a needle valve. Passing a Teflon capillary of 0.7–1.0 mm in diameter directly after the discharge, the atoms are guided

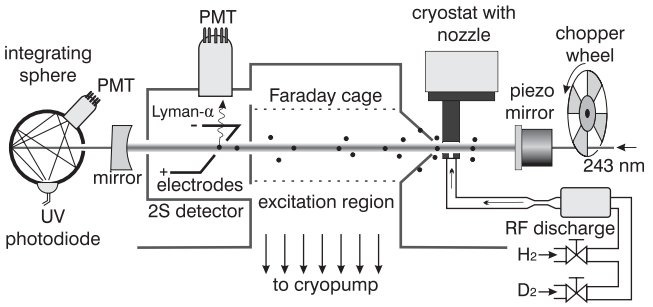


FIG. 2. Excitation region for two-photon spectroscopy on the H/D atomic beam.

by Teflon tubing and thermalize at a copper nozzle (2 mm in diameter) cooled by a liquid helium flow cryostat. The maximum number of atoms is observed for nozzle temperatures of 5.5 K for H and 7.5 K for D. The cold atomic beam is defined by two apertures at the beginning and the end of the excitation zone which is differentially pumped by a cryogenic pump and surrounded by a Faraday cage. All parts surrounding the excitation zone are covered with graphite to suppress stray electric fields. For detection we mix the excited atoms' $2S$ state with the fast decaying $2P$ states with a small electric field in front of a solar blind photo multiplier tube (PMT) that records the prompt emission of a 121 nm photon. A magnetic field of 5 G is applied to shift the magnetic field sensitive hyperfine components out of the laser scanning range.

Chopping the excitation light at 160 Hz with a 50% duty cycle allows us to select the signal from the slow atoms: After the light has been turned off by the chopper, we wait for a delay $\tau = 10, 210, \ldots, 2210$ $\mu$s to let the fast atoms escape the detector. Thus, lines recorded with higher delay $\tau$ exhibit a smaller second-order Doppler effect at the expense of count rate. We use a multichannel scaler to simultaneously record 12 delayed lines [17].

On each measurement day we randomly pick one isotope to start with and record 30–100 $1S - 2S$ spectra during less than 4 h. Then, we promptly switch to the other isotope and record a similar number of lines. To scan over the line the laser probes the transition at optical frequencies in a random order to avoid possible systematics associated with the scan direction. At each laser frequency we alternate between two laser power levels by using a double pass AOM operating in zero diffraction order. The two simultaneously recorded lines allow us to cancel the ac Stark shift (see below). In total we recorded 3770 lines during 35 d of measurement.

We now consider the major systematic contributions and error budget for our setup. The recorded time-delayed spectra at each delay $\tau$ are fitted by a Lorentzian, in order to assess the second-order Doppler effect. For small $\tau$ the line is strongly asymmetric but the asymmetry gradually vanishes for larger delays as the velocity distribution of the contributing atoms becomes more narrow. The delay $\tau = 1410$ $\mu$s is suitable for further analysis, as it has a small

Doppler effect while still providing a strong signal with good statistics. A Monte Carlo (MC) simulation [18] shows that the frequency shift for the delay 1410 $\mu$s equals $-20$ Hz and is largely independent of the particle mass $m$ and the beam temperature $T$ and thus cancels when the H-D frequencies are subtracted. As has been observed before [17], incomplete thermalization, geometry, and other effects may alter the velocity distribution. These effects may, moreover, depend on the isotope. In order to cover conceivable extreme deviations from the Maxwellian case, we have performed MC simulations with distributions $f(v) \propto v^{2,\ldots,5} \exp(-\frac{mv^2}{2k_BT})$. Here, $v$ is the particle velocity and $k_B$ is Boltzmann's constant. We find an upper bound of 6 Hz for the velocity-distribution-dependent correction. We use this value to estimate the uncertainty due to the line shape.

Although the dc Stark effect is almost identical for both isotopes, it must be analyzed since the two isotopes are measured at different times. For this purpose we replaced the Faraday cage surrounding the excitation region with a plane capacitor with one grounded plate and recorded two lines simultaneously with voltages $\pm V$ applied to the second plate at constant laser power. Reference lines with zero voltage were recorded as well. The dc Stark effect quadratically depends on the electric field strength, and an offset of a fitted parabola from its expected center is associated with stray fields. Repeating the measurement in all three spatial dimensions, we find a corresponding uncertainty of 5 Hz.

The differential H-D ac Stark shift is negligible at our level of accuracy as long as the two isotopes are measured at the same laser power. We therefore monitor the 243 nm cavity transmission with a photodiode and a PMT both connected to an integrating sphere to largely reduce beam pointing effects. We fit the transition frequencies for both isotopes recorded at different laser powers by two parallel lines. The distances between these lines for each day of measurement are given in Fig. 3. As evident from Fig. 3, the day-to-day scatter of the data decreases for the second run. This is mainly due to improved statistics because the continuous counters allow a larger data rate. An uncertainty of 1 Hz is added due to a possible nonlinearity of the power measurement.

Intrabeam atomic collisions may lead to a pressure shift of the hydrogen and deuterium lines, and thermalization effects may also depend on the particle density. The data shown in Fig. 3 (left) are recorded at the lowest possible discharge pressure of $p \approx 1$ mbar, which corresponds to a flow of $1.5 \times 10^{18}$ s$^{-1}$ for $H_2/D_2$ (termed "regular flow"). Under these conditions about $10^{17}$ particles per second leave the nozzle in the interaction region (the rest freezes on the nozzle). This corresponds to a pressure in the nozzle of $10^{-4}$ mbar. Using the MC simulation and the pressure shift coefficient of $-8(2)$ MHz/mbar [19,20], we expect a pressure shift for each of the isotopes of $-3$ Hz for delay 1410 $\mu$s. Averaging the data recorded at regular flow, we

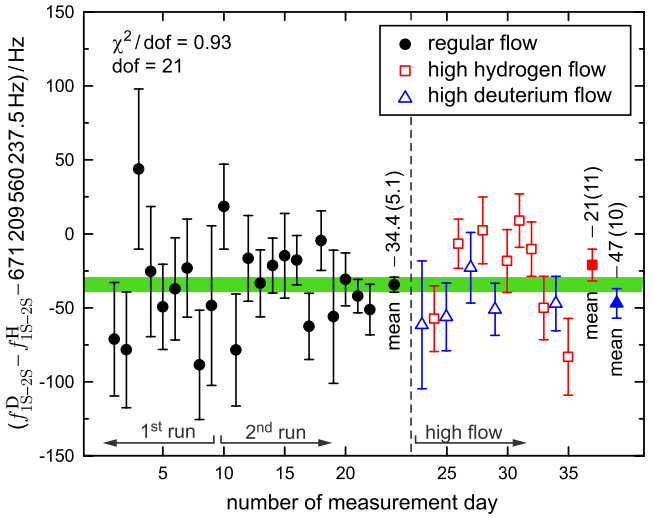


FIG. 3 (color online). $f^D_{1S-2S} - f^H_{1S-2S}$ vs measurement day for $\tau = 1410$ $\mu$s *not* corrected for $\Delta f_{\text{HFS}}$. The error bars show the statistical uncertainty, and the shaded band is the $1\sigma$ uncertainty of the mean for the regular flow data. The full vertical axis corresponds to the $1\sigma$ uncertainty of the previous measurement [4]. The data taken at higher discharge pressures are shown on the right.

obtain $f^D_{1S-2S} - f^H_{1S-2S} = 671\,209\,560\,203.1(5.1)$ Hz, where $\sigma_0 = 5.1$ Hz is the statistical uncertainty. We also measure the isotope shift at $H_2/D_2$ flows increased by a factor of $\sim$3 while maintaining the other isotope flow at the regular level [see Fig. 3 (right)].

In order to investigate density effects experimentally, we perform a two-parameter linear extrapolation to zero flow, which gives $f(p_H, p_D) = f^D_{1S-2S} - f^H_{1S-2S} - [11(11) + 9.7(5.1)p_H - 1.7(4.9)p_D]$ Hz with partial pressures measured at the discharge in mbar. The 11 Hz uncertainty obtained by regression analysis is of the same order as $2\sigma_0$. Thus, the difference $f(0,0) - (f^D_{1S-2S} - f^H_{1S-2S}) = -11(11)$ Hz does not significantly deviate from zero. We therefore keep the mean value of $f^D_{1S-2S} - f^H_{1S-2S}$ as our final experimental result and add an uncertainty of 11 Hz due to density effects.

The uncertainties are summarized as follows: From statistics we have 5.1 Hz, from the hyperfine correction we add 2.9 Hz, from the ac Stark shift at the reference intensity we have 1 Hz, the second-order Doppler effect contributes 6 Hz, and the dc Stark effect gives an additional uncertainty of 5 Hz. Together with the 11 Hz from the density effects, this gives

$$\Delta f_{\text{exp}} = 670\,994\,334\,606(15)\ \text{Hz} \qquad (1)$$

as our final experimental result, confirming and improving the previous measurement [4] by a factor of 10.

According to Refs. [4,7,21], the theoretical contributions to the H-D isotope shift can be classified as (i) differences in the Dirac energy and Barker-Glover corrections [22], (ii) differences in the Lamb shifts, (iii) higher-order nuclear-size and nuclear polarizability corrections, and,

finally, (iv) the main nuclear-size effect given by

$$\Delta E_{\mathrm{iv}} = \left(\frac{1}{1+m/M}\right)^3 \frac{2\alpha^4 c^4 m^3 \langle r^2\rangle}{3n^3\hbar^2}, \tag{2}$$

where $\alpha$ is the fine-structure constant, $m$ is the mass of the orbiting lepton, and $M$ and $\langle r^2\rangle$ are the nuclear mass and the nuclear mean square charge radius, respectively. Following atomic physics conventions and in accordance with the definition of the nuclear radii used in our previous analysis [3,4], we exclude the Barker-Glover corrections as well as the Darwin-Foldy term (which contributes 11.37 kHz to the isotope shift [23]) from the nuclear-size effects. From a nuclear physics point of view [see the paragraph below Eq. (10d) on p. 4582 of Ref. [24]], this convention corresponds to the mean square charge radius difference $\langle r^2\rangle_d - \langle r^2\rangle_p = \langle r^2\rangle_{\mathrm{ch}} - \langle r^2\rangle_E^p$, where $\langle r^2\rangle_{\mathrm{ch}}$ is the mean square radius of the charge distribution of the deuteron and $\langle r^2\rangle_E^p$ is the charge radius of the proton defined via the slope of the Sachs form factor, i.e., $\langle r^2\rangle_E^p = 6\partial G_E(q^2)/\partial q^2|_{q^2=0}$. The conversion of these radii to nuclear physics conventions is discussed in Ref. [24].

The theoretical isotope shift excluding $\Delta E_{\mathrm{iv}}$, i.e., the shift obtained from groups (i) + (ii) + (iii), is obtained as

$$\Delta f_{\mathrm{th}} = 670\,999\,566.90(66)(60)\ \mathrm{kHz}. \tag{3}$$

The current experimental values for the proton-to-electron and deuteron-to-electron mass ratios $M_p/m_e$ and $M_d/m_e$ as given in Ref. [6] yield the first 0.66 kHz uncertainty in Eq. (3), due to their influence on the Dirac energy. The second theoretical uncertainty is due to sets (ii) + (iii). Higher-order recoil terms of order $(Z\alpha)^7(m/M)\times \log(Z\alpha)^{-2}$ and higher-order radiative-recoil corrections contribute 0.34 kHz. In our evaluation, we use the result given in Ref. [25] for the radiative recoil of order $\alpha(Z\alpha)^5 m_e c^2$. The deuteron polarizability is determined according to [9]. Here, we take into account a larger uncertainty of 0.5 kHz in order to account for the possibility of nuclear polarizability effects in diagrams with inelastic multiphoton exchanges according to Refs. [4,7,8,26]. The logarithmic divergence of the form factor is subtracted according to Eq. (69) of Ref. [7].

The difference of the experimental and theoretical values, $\Delta f_{\mathrm{th}} - \Delta f_{\mathrm{exp}} = 5232.29(89)$ kHz, is associated exclusively with $\Delta E_{\mathrm{iv}}$, and the result

$$\langle r^2\rangle_d - \langle r^2\rangle_p = 3.820\,07(65)\ \mathrm{fm}^2 \tag{4}$$

confirms the result of Ref. [4] and constitutes a more than twofold improvement in accuracy. We find that the uncertainty is dominated by the experimental uncertainties of the $M_p/m_e$ and $M_d/m_e$ mass ratios as well as the theoretical uncertainty in the nuclear structure effects, while the measurement of the isotope shift exceeds the accuracy currently needed. Considering the recent developments in cooling techniques [27,28], further experimental improvements on the isotope shift are to be expected. Complementing this conceivable progress, more accurate calculations of nuclear structure effects including multiphoton exchange diagrams and improved measurements of mass ratios are clearly needed.

We acknowledge insightful discussions with K. Pachucki and thank B. Bernhardt, K. Predehl, T. Wilken, and R. Holzwarth for experimental support. J. A. acknowledges support from a Marie Curie Intra European grant, U. D. J. from NSF and NIST (precision measurement grant), N. K. from RSSF and Grant No. MD-887.2008.2, and T. W. H. from the Max Planck Foundation.

*Also at P. N. Lebedev Institute, Moscow, Russia. kolik@lebedev.ru

†Also at Ludwig-Maximilians-University, Munich, Germany.

[1] I. Sick *et al.*, Nucl. Phys. **A637**, 559 (1998).
[2] F. Schmidt-Kaler *et al.*, Phys. Rev. Lett. **70**, 2261 (1993).
[3] K. Pachucki *et al.*, J. Phys. B **29**, 177 (1996).
[4] A. Huber *et al.*, Phys. Rev. Lett. **80**, 468 (1998).
[5] R. Pohl *et al.*, Nature (London) (to be published).
[6] P. J. Mohr *et al.*, Rev. Mod. Phys. **80**, 633 (2008).
[7] K. Pachucki, Phys. Rev. A **52**, 1079 (1995).
[8] M. Puchalski and K. Pachucki, Phys. Rev. A **78**, 052511 (2008).
[9] J. L. Friar, J. Martorell, and D. W. L. Sprung, Phys. Rev. A **59**, 4061 (1999).
[10] L. Essen *et al.*, Nature (London) **229**, 110 (1971).
[11] J. D. Wineland *et al.*, Phys. Rev. A **5**, 821 (1972).
[12] N. Kolachevsky *et al.*, Phys. Rev. A **70**, 062503 (2004).
[13] N. Kolachevsky *et al.*, Phys. Rev. Lett. **102**, 213002 (2009).
[14] J. Alnis *et al.*, Phys. Rev. A **77**, 053809 (2008).
[15] E. Benkler *et al.*, Opt. Express **13**, 5662 (2005).
[16] M. Fischer *et al.*, Phys. Rev. Lett. **92**, 230802 (2004).
[17] A. Huber *et al.*, Phys. Rev. A **59**, 1844 (1999).
[18] N. Kolachevsky *et al.*, Phys. Rev. A **74**, 052504 (2006).
[19] D. H. McIntyre *et al.*, Phys. Rev. A **41**, 4632 (1990).
[20] T. C. Killian *et al.*, Phys. Rev. Lett. **81**, 3807 (1998).
[21] M. I. Eides *et al.*, Phys. Rep. **342**, 63 (2001).
[22] W. A. Barker and F. N. Glover, Phys. Rev. **99**, 317 (1955).
[23] K. Pachucki and S. G. Karshenboim, J. Phys. B **28**, L221 (1995).
[24] J. L. Friar, J. Martorell, and D. W. L. Sprung, Phys. Rev. A **56**, 4579 (1997).
[25] A. Czarnecki *et al.*, Phys. Rev. Lett. **87**, 013001 (2001); M. I. Eides *et al.*, Phys. Rev. A **63**, 052509 (2001); K. Pachucki, Phys. Rev. A **52**, 1079 (1995).
[26] K. Pachucki (private communication).
[27] N. Vanhaecke *et al.*, Phys. Rev. A **75**, 031402(R) (2007).
[28] E. Narevicius *et al.*, Phys. Rev. Lett. **100**, 093003 (2008).